ELSEVIER

Biophysical Chemistry 96 (2002) 191–201

Biophysical Chemistry

www.elsevier.com/locate/bpc

# Thermodynamics of the coil–α-helix transition of amphipathic peptides in a membrane environment: the role of vesicle curvature☆

Torsten Wieprecht[a,1], Michael Beyermann[b], Joachim Seelig[a,*]

[a]*Department of Biophysical Chemistry, Biozentrum University of Basel, Klingelbergstrasse 70, CH-4056 Basel, Switzerland*
[b]*Institute of Molecular Pharmacology, Alfred-Kowalke-Str. 4, D-10315 Berlin, Germany*

Received 19 June 2001; received in revised form 2 October 2001; accepted 5 October 2001

**Abstract**

The binding of peptides or proteins to a bilayer membrane is often coupled with a random coil→α-helix transition. Knowledge of the energetics of this membrane-induced folding event is essential for the understanding of the mechanism of membrane activity. In a recent study [Wieprecht et al., J. Mol. Biol. 294 (1999) 785–794], we have developed an approach which allows an analysis of the energetics of membrane-induced folding. We have systematically varied the helix content of the amphipathic peptide magainin-2-amide by synthesizing analogs where two adjacent amino acid residues were substituted by their corresponding D-enantiomers and have measured their binding to small unilamellar vesicles (SUVs). Correlation of the binding parameters with the helicities allowed the evaluation of the thermodynamic parameters of helix formation. Since SUVs (30 nm in diameter) are characterized by a non-ideal lipid packing due to their high membrane curvature, we have now extended our studies to large unilamellar vesicles (LUVs) (100 nm in diameter) with a lipid packing close to planar membranes. While the free energy of binding was similar for SUVs and LUVs, the binding enthalpies and entropies were distinctly different for the two membrane systems. The thermodynamic parameters of the coil–helix transition were nevertheless not affected by the vesicle size. Helix formation at the membrane surface of LUVs (SUVs) was characterized by an enthalpy change of −0.8 (−0.7) kcal/mol per residue, an entropy change of −2.3 (−1.9) cal/mol K per residue, and a free energy change of −0.12 (−0.14) kcal/mol per residue. Helix formation accounted for ∼50% of the free energy of binding underlining its major role as a driving force for membrane-binding. 

*Keywords:* Helix–coil transition; Amphipathic peptide; Peptide–membrane interaction; Titration calorimetry; Magainin

*Abbreviations:* M2a, magainin 2 amide; ITC, isothermal titration calorimetry; SUVs, small unilamellar vesicles; LUVs, large unilamellar vesicles; POPC, 1-palmitoyl-2-oleoyl phosphatidylcholine; POPG, 1-palmitoyl-2-oleoylphosphatidyl-DL-glycerol; CD, circular dichroism; Tris, tris(hydroxymethyl) aminomethane.

☆ Supported by the Swiss National Science Foundation Grant #31-5880.

*Corresponding author. Tel.: +41-61-267-2190; fax: +41-61-267-2189.
*E-mail address:* joachim.seelig@unibas.ch (J. Seelig).
[1] Present address: Ciba Speciality Chemicals, P.O. Box 1266, D-79639 Grenzach-Wyhlen, Germany.

0301-4622/02/$ - see front matter 
PII: S0301-4622(02)00025-X

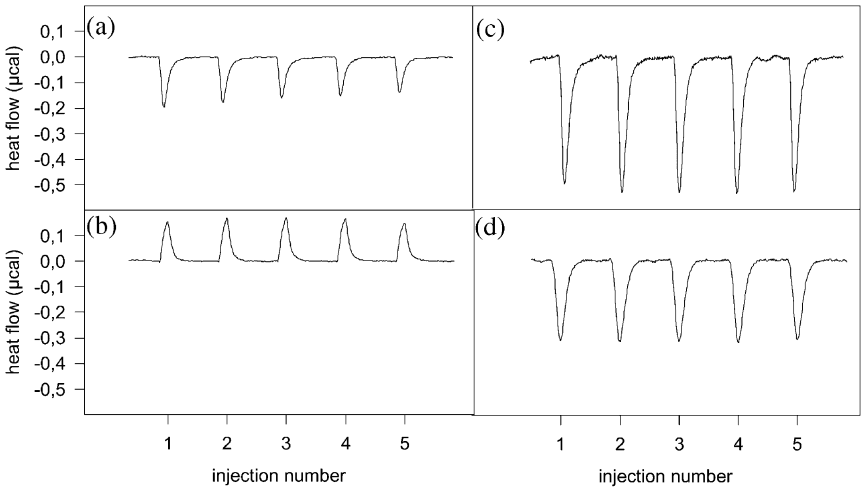


Fig. 1. Calorimeter traces of the injection of M2a (a,c) and d11,12 M2a (b,d) into POPC/POPG (3:1) LUVs (a,b) or SUVs (c,d) at 30 °C. The specific conditions were: (a) injection of 7 μl of 200 μM M2a into 20 mM POPC/POPG (3:1) LUVs; (b) injection of 7 μl of 200 μM d11,12 M2a into 20 mM POPC/POPG (3:1) LUVs; (c) injection of 5 μl of 200 μM M2a into 20 mM POPC/POPG (3:1) SUVs; (d) injection of 6 μl of 200 μM d11,12 M2a into 17.5 mM POPC/POPG (3:1) LUVs.

## 1. Introduction

The potential of a peptide to assume an α-helical conformation is generally higher in a hydrophobic environment than in water since the water molecules destabilize the intra-molecular hydrogen bonds of the helix [2,3]. The binding of peptides/proteins to biological membranes corresponds to a transfer from the aqueous phase to a hydrophobic phase and is frequently accompanied by a conformational transition from a random coil conformation to an α-helix. Typical examples exhibiting such a transition are signal peptides, apolipoproteins, virus fusion peptides and membrane-lytic antimicrobial peptides [4–13].

The thermodynamics of the α-helix formation in water has been extensively investigated. Helix formation was found to be driven by a negative enthalpy, $\Delta H_{\text{helix}}$, of −0.9 to −1.3 kcal/mol per residue and opposed by a negative entropy, $\Delta S_{\text{helix}}$, of −2.5 to −4.6 cal/mol K per residue [14–20]. $\Delta H_{\text{helix}}$ was largely independent of the peptide sequence and was suggested to reflect mainly differences in the enthalpic states between intra- and intermolecular hydrogen bonds [16,20].

Thermodynamic data on the *membrane-induced* random coil → α-helix transition are scarce. The only three peptides studied so far are the bee venom melittin [21] the antimicrobial peptide magainin 2 amide (M2a) [1] and the signal sequence of mitochondrial rhodenese (RHD) [22]. The thermodynamic analysis was made possible by the synthesis of a set of peptides with the same primary sequence but with two adjacent amino acids substituted by the corresponding D-enantiomers. Double-D-substitution leads to a local disturbance of the helical conformation, but does not modify other important properties such as overall hydrophobicity and side-chain functionality [13,23]. We have measured the thermodynamic parameters of the binding of these peptides to negatively-charged 1 - palmitoyl - 2 - oleoyl - *sn* - glycero - 3 - phosphocholine/1 - palmitoyl - 2 - oleoyl - *sn* - glycero - 3 - phosphoglycerol [POPC/POPG (3:1)] sonicated vesicles (small unilamellar vesicles — SUVs) with isothermal titration calorimetry (ITC) and have correlated them with the peptide helicities in the membrane-bound state. A linear relationship between the relevant thermodynamic parameters and the extent of helix formation could be observed. From the slopes of the linear regression lines the contribution of helix formation to the overall binding process could be

derived. In the case of M2a, helix-formation was accompanied by an enthalpy change of $\Delta H_{helix} = -0.7$ kcal/mol per residue, an entropy change of $\Delta S_{helix} = -1.9$ cal/mol K per residue and a free energy change of $\Delta G_{helix} = -0.14$ kcal/mol per residue.

In the course of our studies, we have compared binding of M2a to small and to large unilamellar vesicles at 45 °C (SUVs, LUVs) [24]. SUVs are prepared by sonication and have a mean diameter of ~30 nm. They are considerably curved, resulting in less dense packing of the phospholipids. In contrast, LUVs are prepared by extrusion through polycarbonate filters, have a larger diameter of ~100 nm and their lipid packing density is close to that of planar membranes. SUVs offer experimental advantages in spectroscopic studies (reduced light scattering), but LUVs are probably the system of choice most closely related to biological membranes. Binding studies with M2a revealed almost identical free energies of binding to LUVs and SUVs at 45 °C. However, both the enthalpy and the entropy of binding were distinctly more positive for LUVs ($\Delta H^0 = -3.6$ kcal/mol; $\Delta S^0 = +8.0$ cal/mol K) than for SUVs ($\Delta H^0 = -9.2$ kcal/mol; $\Delta S^0 = -9.6$ cal/mol K) [24]. The molecular origin of these dramatic differences in $\Delta H^0$ and $\Delta S^0$ was not explained and it could indeed be argued that helix formation to SUVs and LUVs is characterized by different sets of thermodynamic parameters.

In the present study, we have therefore extended our approach of double-D substitution to large unilamellar vesicles, using again M2a and three isomers (d4,5 M2a, d11,12 M2a and d16,17 M2a). We have determined the enthalpy of binding as well as the binding isotherms to POPC/POPG (3:1) LUVs (100 nm) with high sensitivity isothermal titration calorimetry and have correlated the thermodynamic binding parameters with the helicity.

## 2. Materials and methods

### 2.1. Materials

POPC and POPG were purchased from Avanti Polar Lipids, Inc., Alabaster, AL, USA. The Fmoc amino acids for peptide synthesis were obtained from Novabiochem, Bad Soden, Germany. All other chemicals were of analytical or reagent grade. The buffer was prepared from 18 MΩ water obtained from a NANOpure A filtration system.

### 2.2. Peptide synthesis

The peptide investigated was the antibacterial frog peptide magainin-2-amide (M2a) with the sequence GIGKF LHSAK KFGKA FVGEI MNS($NH_2$). M2a and its double-D-isomers d4,5 M2a, d11,12 M2a, and d16,17 M2a were synthesized by solid-phase methods using standard Fmoc chemistry on Tenta Gel S RAM resin (0.21 mmol/g; RAPP Polymere, Tübingen, Germany) in the continuous-flow mode on a MilliGen 9050 (Millipore, MA, USA) peptide synthesizer. Purification was carried out by preparative high-performance liquid chromatography (HPLC) on PolyEncap A300, 10 μm (250×20 mm i.d.) (Bischoff Analysentechnik GmbH, Leonberg, Germany) to give final products >95% pure by HPLC analysis. All peptides were characterized by matrix-assisted laser desorption ionization mass spectrometry (MALDI II; Kratos, Manchester, UK) with peptide content of lyophilized samples being determined by quantitative amino acid analysis (LC 3000, Biotronik-Eppendorf, Germany).

### 2.3. Preparation of lipid vesicles

A defined amount of lipid in chloroform was first dried under a nitrogen stream. The lipid was then dissolved in dichloromethane and again dried under nitrogen and subsequently overnight under high vacuum. Typically, 2–3 ml buffer [10 mM tris(hydroxymethyl)-aminomethane (Tris), 100 mM NaCl, pH 7.4] were added to the lipid and the dispersion was extensively vortexed. LUVs were prepared by the extrusion technique [25]. The lipid suspension was frozen and thawed in liquid nitrogen (six times) and then extruded 10 times through 0.1 μm polycarbonate filters. The lipid concentration was calculated on basis of the weight of the dried lipid. The data for small unilamellar vesicles were taken from previous publications [1,24].

### 2.4. High sensitivity titration calorimetry

Isothermal titration calorimetry was performed using a VP high-sensitivity titration calorimeter (Microcal, Northampton, MA, USA) [26]. Solutions were degassed under vacuum prior to use. The heat of dilution values were determined in control experiments by injecting either the peptide solution or the lipid suspension into buffer (10 mM Tris, 100 mM NaCl, pH 7.4). The heats of dilution were subtracted from the heats determined in the corresponding peptide-lipid binding experiments. All experiments were performed at 30 °C.

### 2.5. Circular dichroism spectroscopy

CD measurements were carried out on SUVs with a Jasco 720 spectrometer between 200–260 nm at 30 °C. The helicity of the peptides, $f_h$, was determined from the mean residue ellipticity $[\Theta]$ at 222 nm as described by Scholtz et al. [19]:

$$f_h = \frac{[\Theta]_{222} - [\Theta]_{coil}}{[\Theta]_{helix} - [\Theta]_{coil}}$$

$$[\Theta]_{helix} = -40\,000(1 - 2.5/n) + 100t$$

$$[\Theta]_{coil} = 640 - 45t$$

where $[\Theta]_{222}$ is the measured mean residue ellipticity at 222 nm expressed in degrees $cm^2$ $dmol^{-1}$, $[\Theta]_{helix}$ and $[\Theta]_{coil}$ are the mean residue ellipticities of the completely helical and completely coiled form of the peptide (at 222 nm, expressed in degree $cm^2$ $dmol^{-1}$), respectively, $n$ is the number of amino acid residues and $t$ is the temperature in °C. The quality of the CD spectra of LUVs was not sufficient to allow an evaluation of the helix content (large perturbations due to light scattering). The same helix content was assumed as determined for SUVs.

## 3. Results

### 3.1. Thermodynamics of peptide binding

The enthalpy change upon binding of M2a and its analogs to lipid vesicles could be measured with high-sensitivity isothermal titration calorimetry in a single experiment by injecting small aliquots of a peptide solution into a vesicle suspension of high lipid concentration (peptide-to-lipid titration, cf. [27]). The lipid concentration in the calorimeter cell was much larger than the injected peptide concentration leading to an almost complete binding of the added peptide. Fig. 1a shows the result of the injection of 7 μl aliquots of a 200-μM M2a solution (buffer: 10 mM Tris, 100 mM NaCl, pH 7.4) into 20 mM POPC/POPG (3:1) LUVs (same buffer) at 30 °C. Fig. 1b shows the analogous experiment performed with d11,12 M2a. The average heats of reaction observed after subtraction of the heat of dilution (measured in control experiments of the injection of peptide into buffer) were −3.8 μcal for M2a and +7.3 μcal for d11,12 M2a. While the binding of the helical M2a was exothermic, binding of the less helical d11,12 M2a was distinctly endothermic. Dividing the heat of reaction by the amount of injected peptide (1.4 nmol) yields the molar enthalpy of binding, $\Delta H^0$. $\Delta H^0$ comprises the binding step proper and the enthalpic contribution of helix formation. Under the present conditions, more than 93% of the injected peptide was bound to the LUVs as was calculated from the binding isotherms (cf. below). The binding enthalpies of all peptides, corrected for 100% binding are summarized in Table 1. Fig. 1 also displays the calorimeter tracings of the corresponding experiments performed with small unilamellar vesicles prepared by sonication (Fig. 1c,d). The $\Delta H^0$ obtained with SUVs were always exothermic and considerably larger in absolute value than those measured for SUVs (cf. Table 1). However, the two sets of data agree in so far as the binding enthalpies increase in the order M2a < d4,5 M2a < d16,17 M2a < d11,12 M2a.

In a second type of experiment, the peptide was contained in the calorimeter cell and lipid vesicles were injected (lipid-to-peptide titration [27]). This allowed the determination of binding isotherms for the binding of M2a, d11,12 M2a and d16,17 M2a to POPC/POPG (3:1) to LUVs. The same approach was, however, unsuccessful for d4,5 M2a since the binding enthalpy of this analog ($\Delta H^0 =$ 0.7 kcal/mol) was too small for a reliable determination of the binding isotherm. Typical binding

Table 1
Thermodynamic parameters for the binding of M2a peptides to POPC/POPG (3:1) SUVs and LUVs at 30 °C

| Peptide | $\Delta H^0$ (kcal/mol)[b] | | $\Delta G^0$ (kcal/mol)[b] | | $\Delta S^0$ (cal/mol K) | | Helicity[a] (%) |
|---|---|---|---|---|---|---|---|
| | SUVs[a] | LUVs | SUVs[a] | LUVs | SUVs[a] | LUVs | |
| M2a | $-17.0\pm1.0$ | $-3.0\pm0.3$ | $-4.8\pm0.1$ | $-4.0\pm0.1$ | $-40.3\pm3.6$ | $3.2\pm1.4$ | 74 |
| d4,5 M2a | $-13.0\pm0.9$ | $0.7\pm0.1$ | $-4.0\pm0.1$ | $(-3.5)$[c] | $-29.7\pm3.3$ | $(13.9)$[c] | 53 |
| d16,17 M2a | $-12.3\pm0.5$ | $2.8\pm0.2$ | $-3.6\pm0.1$ | $-3.1\pm0.2$ | $-28.6\pm2.0$ | $19.5\pm1.4$ | 41 |
| d11,12 M2a | $-9.1\pm0.6$ | $5.3\pm0.1$ | $-3.4\pm0.1$ | $-2.8\pm0.1$ | $-18.8\pm2.3$ | $26.9\pm0.8$ | 29 |

[a] Thermodynamic parameters for SUVs and helicities were taken from Wieprecht et al. [1].
[b] $\Delta H^0$ and $\Delta G^0$ were determined from at least two independent peptide-to-lipid or lipid-to-peptide titration experiments, respectively.
[c] $\Delta G^0$ and $\Delta S^0$ for d4,5 M2a binding to LUVs were not determined experimentally. Numbers in parentheses were calculated from the corresponding regression Eqs. (5) and (6).

experiments are shown in Fig. 2. The peptide was employed at μM concentrations (Fig. 2a: 7 μM M2a, Fig. 2c: 10 μM d16,17 M2a, Fig. 2e: 10 μM d11,12 M2a) and each titration peak corresponds to a 20-μl injection of a 30-mM POPC/POPG (3:1) LUV suspension. Fig. 2 shows that the amount of heat released or absorbed decreases with increasing injection number as less and less peptide remains free in solution. The heat of reaction values are shown in Fig. 2b,d,f after subtraction of the heats of dilution obtained in control experiments of vesicle-into-buffer titrations. For M2a, the heat of reaction values approach zero after approximately seven injections; for d11,12, and d16,17 M2a approximately 14 injections are needed. From these measurements, the binding isotherms, i.e. the dependence of the molar ratio of bound peptide per total lipid, $X_b$, on the free peptide concentration in solution, $C_f$, can be derived using the established procedures (Fig. 3) [27]. $X_b$ has been calculated on basis of the lipid present in the outer leaflet of the bilayer only since the peptides cannot cross the bilayer under the present experimental conditions. Our results show that binding affinity of M2a and its analogs to LUVs decreases in the same order as previously found for SUVs, i.e. M2a > d16,17 M2a > d11,12 M2a (d4,5 M2a — not determined).

The quantitative analysis of the binding isotherms in terms of binding constants and binding affinities requires the assumptions of a specific binding model. The model employed in this study is a surface partition equilibrium with the specific condition that peptide partitioning/binding is linearly related to the peptide concentration immediately above the membrane surface, i.e. the surface concentration $C_M$:

$$X_b = KC_M \quad (1)$$

The surface concentration $C_M$ depends on (i) the free peptide concentration in bulk solution $C_f$; (ii) on the membrane surface charge density; and (iii) on the peptide charge. POPC/POPG (3:1) vesicles possess a negative surface potential of approximately −50 mV in the present buffer, resulting in an attraction of the positively charged peptides (electric charge $z \sim 3.5$) to the membrane surface. As a consequence, the peptide surface concentration ($C_M$) is enhanced compared to that in bulk solution ($C_f$). Using the Gouy–Chapman theory (for reviews see: [28,29]) it is possible to calculate $C_M$ for each data point of the binding isotherm and, in turn, to determine the binding constant $K$. A detailed description of this binding model as applied to magainin peptides has been given elsewhere [30,31]. Using the same model, we have simulated the calorimetric data and the binding isotherms. The solid lines in Fig. 2 (right panels) and Fig. 3 show the best theoretical fits. Good agreement between theory and experiment was obtained with $K = 15\ M^{-1}$ for M2a, $K = 4\ M^{-1}$ for d16,17 M2a and $K = 2.2\ M^{-1}$ for d11,12 M2a. These binding constants exclusively describe the hydrophobic interaction with the membrane since the electrostatic attraction has been corrected for by using the Gouy–Chapman theory.

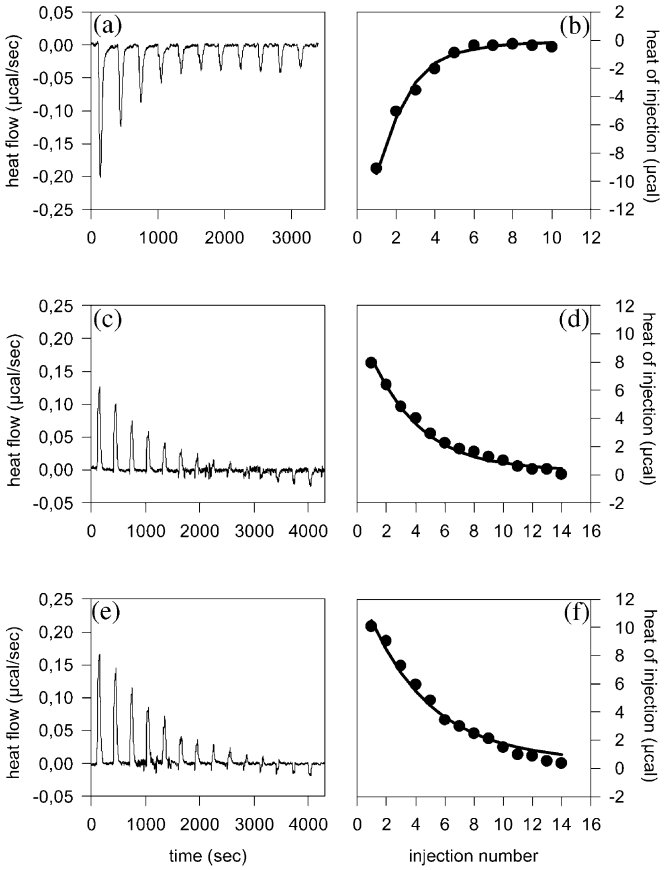


Fig. 2. Titration calorimetry of peptide solutions with POPC/POPG (3:1) LUVs at 30 °C. The panels on the left show the calorimetric tracings for (a) the injection of 20 μl of 30 mM POPC/POPG (3:1) LUVs into 7 μM M2a, (c) the injection of 20 μl of 30 mM POPC/POPG (3:1) LUVs into 10 μM d16,17 M2a, and (e) the injection of 20 μl of 30 mM POPC/POPG (3:1) LUVs into 10 μM d11,12 M2a. The panels on the right show the corresponding heats of reaction after subtraction of the heats of dilution measured in lipid-to-buffer control experiments. The solid lines correspond to the best fit of the experimental data points using a model which combines a surface partition equilibrium with the Gouy–Chapman theory. The specific fit parameters are: (b) M2a: $K=15\ M^{-1}$, $\Delta H=-2.3$ kcal/mol; (d) d16,17 M2a: $K=4\ M^{-1}$, $\Delta H=2.9$ kcal/mol and (f) d11,12 M2a: $K=2.2\ M^{-1}$, $\Delta H=5.0$ kcal/mol.

The standard free energies for the transfer of the peptide from the lipid–water interface into the membrane $\Delta G^0$ can be calculated according to:

$$\Delta G^0 = -RT\ln 55.5K \quad (2)$$

where $RT$ is the thermal energy and 55.5 is the molar concentration of water, correcting for the cratic contribution [32]. The free energies of binding of the different M2a analogs to LUVs (this work) and SUVs [1] are summarized in Table 1.

Finally, the entropy of binding $\Delta S^0$ can be calculated using the relation:

$$\Delta G^0 = \Delta H^0 - T\Delta S^0 \quad (3)$$

The $\Delta S^0$ values are also listed in Table 1.

### 3.2. Correlation between thermodynamic parameters and helicity

The helicity of M2a and its double-D-isomers in the membrane-bound state was previously measured by means of circular dichroism spectroscopy [1]. The helicity was found to decrease in the order M2a (74%) > d4,5 M2a (53%) > d16,17 M2a (41%) > d11,12 M2a (29%). The correlation

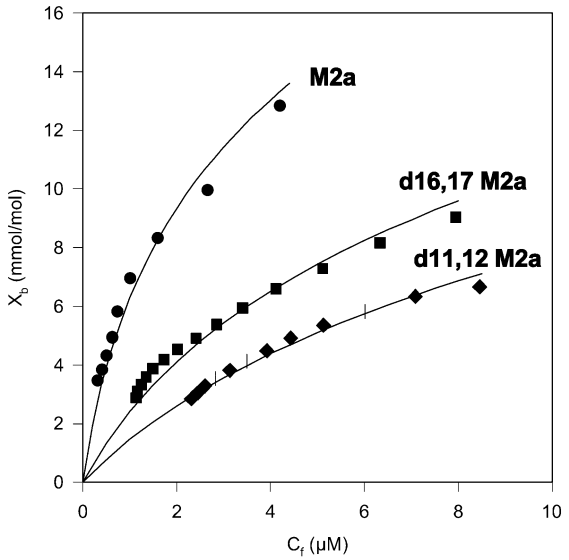


Fig. 3. Binding isotherms of M2a and its double-D-isomers obtained for POPC/POPG (3:1) LUVs at 30 °C. $X_b$ is the molar ratio of bound peptide per total lipid calculated on the basis of the accessible lipid present in the outer layer of the LUVs (50%). The solid lines correspond to the theoretical binding isotherms calculated by combining a surface partition equilibrium with the Gouy–Chapman theory. The binding constants are 15 $M^{-1}$ for M2a, 4 $M^{-1}$ for d16,17 M2a and 2.2 $M^{-1}$ for d11,12 M2a.

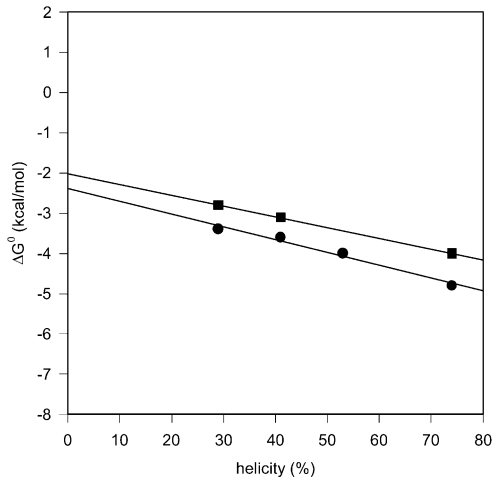


Fig. 5. Variation of the free energy of binding $\Delta G^0$ with the helicity of the peptides in the lipid-bound state at 30 °C: (●) SUVs — data taken from [1]; (■) LUVs.

between the thermodynamic binding parameters and helicity is shown in Figs. 4–6 for both LUVs (this work) and SUVs (data taken from [1]). The figures demonstrate that a linear relation exists between the thermodynamic binding parameters and the helicity. For LUVs the following expressions are derived by translating the percentage

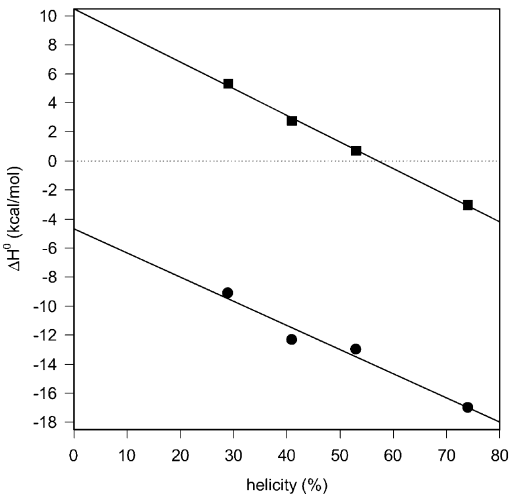


Fig. 4. Variation of the enthalpy of binding $\Delta H^0$ with the helicity of the peptides in the lipid-bound state at 30 °C: (●) SUVs — data taken from [1]; (■) LUVs.

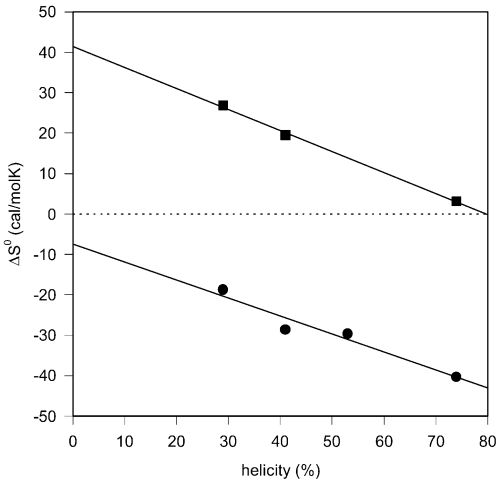


Fig. 6. Variation of the entropy of binding $\Delta S^0$ with the helicity of the peptides in the lipid-bound state at 30 °C: (●) SUVs — data taken from [1]; (■) LUVs.

Table 2
Thermodynamic parameters characteristic for M2a binding to POPC/POPG (3:1) SUVs and LUVs at 30 °C

| | Coil–helix transition[a] | | | Non-helix contribution to binding[b] | | |
|---|---|---|---|---|---|---|
| | $\Delta G_{helix}$ (kcal/mol residue) | $\Delta H_{helix}$ (kcal/mol residue) | $\Delta S_{helix}$ (cal/mol K residue) | $\Delta G_{coil}$ (kcal/mol) | $\Delta H_{coil}$ (kcal/mol) | $\Delta S_{coil}$ (cal/mol K) |
| SUVs[c] | $-0.14\pm0.01$ | $-0.72\pm0.09$ | $-1.93\pm0.33$ | $-2.4\pm0.2$ | $-4.7\pm1.1$ | $-7.4\pm3.9$ |
| LUVs | $-0.12\pm0.01$ | $-0.80\pm0.02$ | $-2.26\pm0.12$ | $-2.0\pm0.1$ | $10.5\pm0.3$ | $41.5\pm1.4$ |

[a] Values were obtained from the slopes of linear regression plots of the binding parameters vs. the helicity.
[b] Values were obtained from the intercepts of linear regression plots Figs. 4–6. They describe the binding of a hypothetical M2a molecule which cannot undergo the coil→α-helix transition.
[c] Data for SUVs were taken from Wieprecht et al. [1].

helicity into number of helical segments, $n_{helix}$:

$$\Delta H^0 = -0.80 n_{helix} + 10.5 \text{ (kcal/mol)} \quad (4)$$

$$\Delta G^0 = -0.12 n_{helix} - 2.0 \text{ (kcal/mol)} \quad (5)$$

$$\Delta S^0 = -2.26 n_{helix} + 41.5 \text{ (cal/mol K)} \quad (6)$$

The slopes of the regression lines yield the thermodynamic parameters of helix formation as $\Delta H^{LUV}_{helix} = -0.80$ kcal/mol per residue, $\Delta G^{LUV}_{helix} = -0.12$ kcal/mol per residue and $\Delta S^{LUV}_{helix} = -2.26$ cal/mol K per residue. These data are very similar to those obtained previously for SUVs (Table 2) revealing the absence of significant differences in the thermodynamics of helix formation of the peptides bound to SUVs or LUVs.

The intercepts with the ordinate can be interpreted as the thermodynamic binding parameters of a hypothetical peptide which does not undergo a conformational transition upon membrane binding and are denoted by the subscript 'coil' in Table 2. They are discussed below.

## 4. Discussion

### 4.1. Thermodynamics of the coil–helix transition

The replacement of two adjacent L-amino acids by their D-enantiomers (double-D substitution) results in a local disturbance of the helix and a reduced overall helicity of the peptide [13,23]. The helix disturbance is likely to occur via a disruption of the intra-molecular hydrogen bond network around the substitution site since the backbone torsion angles typical for a right-handed α-helix are not easily accessible for the D-enantiomers. A correlation of the thermodynamic binding parameters with the helicity is expected to give an approximately linear relation provided the thermodynamic parameters of the coil→α-helix transition are independent of the peptide sequence. This is strictly valid only for homopolymers in an isotropic environment, but has also been shown to be a reasonable approximation for the coil→α-helix transition of M2a and of RHD bound to POPC/POPG (3:1) SUVs [1,22].

An inspection of Fig. 4 and Table 1 reveals large differences between the experimentally observed binding enthalpies of SUVs and LUVs. The binding to LUVs is distinctly more endothermic by approximately $\delta\Delta H^0 = \Delta H^0_{LUV} - \Delta H^0_{SUV} = 14.0$ kcal/mol for all M2a peptides. This phenomenon has been observed before [33,34] and will be discussed in more detail below. For the present purposes, it is important to note that almost the *same* shift occurs for *all* M2a analogs. Hence, a plot of $\Delta H^0_{SUV}$ and $\Delta H^0_{LUV}$ vs. helicity yields straight lines of almost identical slopes but shifted along the ordinate by $\delta\Delta H^0$. From the slopes of the straight lines it is possible to calculate the mean enthalpy of helix formation per residue which is $\Delta H_{helix} = -0.72\pm0.09$ kcal/mol for SUVs and $-0.80\pm0.02$ for LUVs. An enthalpy-driven helix formation is in accordance with results obtained for peptides in water. In water, $\Delta H_{helix}$ is in the range of $-0.9$ to $-1.3$ kcal/mol per residue and is again largely independent of the peptide sequence [14–20]. The enthalpy change is mainly attributed to the formation of intra-molecular hydrogen bonds [16,20]. In the more hydrophobic environment of an aqueous 7 M 2,2,2,-trifluoro-

ethanol solution, $\Delta H^0_{helix}$ is reduced in magnitude to $-0.7$ kcal/mol residue [35], which is in the same range as found for M2a bound to SUVs and LUVs. α-Helix formation in a hydrophobic environment is, therefore, less exothermic than in water. This is also supported by analogous measurements performed with the RHD mitochondrial pre-sequence, again a 23 amino acid amphipathic peptide, where $\Delta H_{helix}$ was $-0.53$ kcal/mol and $-0.63$ kcal/mol residue for SUVs and LUVs, respectively [22].

Helix formation is opposed by entropy. Fig. 6 can be used to determine the incremental entropy per helix segment, $\Delta S_{helix}$. The entropy contribution is negative and amounts to $\Delta S_{helix} = -1.9$ cal/mol K for SUVs and $-2.3$ cal/mol K for LUVs [for comparison RHD: $-0.9$ cal/mol K (SUVs) to $-1.3$ cal/mol K (LUVs)]. In contrast, helix formation in water entails a considerably larger loss of entropy of $-2.5$ to $-4.6$ cal/mol K per residue [15,16,18]. The first step in the membrane-induced helix formation is the adsorption of the peptide to the membrane surface. This limits the conformational freedom of the molecule to a small volume parallel to the membrane surface. Compared to a three-dimensional random walk in aqueous solution, this reduction in dimensionality appears to simplify helix formation and may explain the less negative $\Delta S_{helix}$ observed in membrane-induced helix formation.

As discussed above helix formation in the lipid–water interface is driven by enthalpy but opposed by entropy. The net effect of these opposing forces results in an energetically still favorable free energy change. Linear regression analysis of the data presented in Fig. 5 leads to $\Delta G_{helix} = -0.14$ kcal/mol per residue for SUVs and $-0.12$ kcal/mol for LUVs (for comparison RHD: $-0.2$ kcal/mol (SUVs) to $-0.23$ kcal/mol (LUVs); [22]). The total free energy change of M2a binding to SUVs (LUVs) is $-4.8$ kcal/mol ($-3.0$ kcal/mol). Helix formation contributes 0.74 (helicity) $\times$ 23 (residues) $\times -0.14$ (kcal/mol) $= -2.4$ kcal (LUVs: $-2.0$ kcal/mol), i.e. 50–70% of the total free energy change arises from helix formation. Binding of the same peptides to the lipid membrane without the possibility to fold into an α-helix would lead to a much reduced binding affinity and to hydrophobic binding constants smaller by 1–2 orders of magnitude.

In a recent study, Ladokhin and White [21] investigated the contribution of α-helix formation to the binding thermodynamics of melittin and reported a $\Delta G_{helix}$ of $-0.4$ kcal/mol residue. The authors suggested values of between $-0.4$ and $-0.6$ kcal/mol per residue as reasonable first estimates of the free energy difference between the partitioning of folded and unfolded peptides. This result, based on a single experiment, is obviously quite different from the more extensive set of data derived for M2a and RHD binding to SUVs and LUVs.

The results obtained for M2a (this work) and RHD) [22] demonstrate that α-helix formation induced by SUVs and LUVs is characterized by virtually the same thermodynamic parameters. Moreover, the total free energy of binding, $\Delta G^0$, (including binding and helix formation) is similar in absolute values for LUVs and SUVs (cf. Fig. 5 (this work); [22], Fig. 5). This is in contrast to the large differences measured for the enthalpy $\Delta H^0$ and entropy $\Delta S^0$ as best illustrated by extrapolating the measured $\Delta H^0$, $\Delta G^0$ (derived from $K$), and $\Delta S^0$ to zero helicity (cf. Figs. 4–6). The corresponding thermodynamic parameters are listed in Table 2 as $\Delta H_{coil}$, $\Delta S_{coil}$ and $\Delta G_{coil}$. They describe the binding parameters of a hypothetical peptide which cannot fold at the lipid–water interface. Inspection of Table 2 shows that the free energy of binding, $\Delta G_{coil}$, is almost identical for LUVs and SUVs, but that remarkable differences exist for $\Delta H_{coil}$ and $\Delta S_{coil}$. M2a binding to LUVs is enthalpy-driven ($\Delta H_{coil} = -4.7$ kcal/mol) and opposed by entropy ($\Delta S_{coil} = -7.4$ cal/mol K), whereas for LUVs the enthalpy is unfavorable ($+10.5$ kcal/mol) and the binding is entropy-driven ($\Delta S_{coil} = +41.5$ cal/mol K). Since $\Delta G_{coil}$ remains almost unchanged, the transition from LUVs to SUVs is accompanied by an enthalpy–entropy compensation mechanism. The molecular origin of this effect is not clear. However, it is not unique for M2a peptides but has been observed before for a somatostatin-like peptide, octreotide, which has a cyclic structure and cannot undergo extensive conformational changes upon binding [33]. An entropy–enthalpy compensation between

SUVs and LUVs has further been reported for an Apo-AI model peptide [5,34], the RHD signal sequence [22] and a peptidic detergent, surfactin [36]. In all systems the binding to SUVs is enthalpy-driven whereas the binding to LUVs is entropy-driven. This effect is at present under further investigation.

## 5. Conclusion

Large differences exist in the enthalpy and entropy of binding of the amphipathic peptide magainin 2 amide to SUVs and to LUVs. Nevertheless, the contribution of the coil → α-helix transition to the binding thermodynamics is the same for highly curved and more planar vesicles. For both model systems, helix formation is driven by a negative enthalpy change and opposed by a negative entropy change. The free energy of helix formation accounts for approximately 50% of the binding free energy and helix formation is, hence, a major driving force of the binding reaction.

## References

[1] T. Wieprecht, O. Apostolov, M. Beyermann, J. Seelig, Thermodynamics of the α-helix–coil transition of amphipathic peptides in a membrane environment: implications for the peptide-membrane binding equilibrium, J. Mol. Biol. 294 (1999) 785–794.

[2] M. Blaber, X.J. Zhang, B.W. Matthews, Structural basis of amino acid α-helix propensity, Science 260 (1993) 1637–1640.

[3] C.M. Deber, S.C. Li, Peptides in membranes: helicity and hydrophobicity, Biopolymers 37 (1995) 295–318.

[4] G.M. Anantharamaiah, J.L. Jones, C.G. Brouillette, et al., Studies of synthetic peptide analogs of the amphipathic helix. Structure of complexes with dimyristoyl phosphatidylcholine, J. Biol. Chem. 260 (1985) 10248–10255.

[5] J.A. Gazzara, M.C. Phillips, S. Lund-Katz, et al., Interaction of class A amphipathic helical peptides with phospholipid unilamellar vesicles, J. Lipid Res. 38 (1997) 2134–2146.

[6] P.K. Hammen, D.G. Gorenstein, H. Weiner, Amphiphilicity determines binding properties of three mitochondrial presequences to lipid surfaces, Biochemistry 35 (1996) 3772–3781.

[7] R.C. Keller, J.A. Killian, B. de Kruijff, Anionic phospholipids are essential for α-helix formation of the signal peptide of prePhoE upon interaction with phospholipid vesicles, Biochemistry 31 (1992) 1672–1677.

[8] I. Martin, M.C. Dubois, F. Defrise-Quertain, et al., Correlation between fusogenicity of synthetic modified peptides corresponding to the $NH_2$-terminal extremity of simian immunodeficiency virus gp32 and their mode of insertion into the lipid bilayer: an infrared spectroscopy study, J. Virol. 68 (1994) 1139–1148.

[9] D. Roise, G. Schatz, Mitochondrial presequences, J. Biol. Chem. 263 (1988) 4509–4511.

[10] J.P. Segrest, R.L. Jackson, J.D. Morrisett, A.M. Gotto, A molecular theory of lipid-protein interactions in the plasma lipoproteins, FEBS Lett. 38 (1974) 247–258.

[11] W. van Klompenburg, B. de Kruijff, The role of anionic lipids in protein insertion and translocation in bacterial membranes, J. Membr. Biol. 162 (1998) 1–7.

[12] T. Wieprecht, O. Apostolov, M. Beyermann, J. Seelig, Membrane binding and pore formation of the antibacterial peptide PGLa: thermodynamic and mechanistic aspects, Biochemistry 39 (2000) 442–452.

[13] T. Wieprecht, M. Dathe, M. Schumann, E. Krause, M. Beyermann, M. Bienert, Conformational and functional study of magainin 2 in model membrane environments using the new approach of systematic double-D-amino acid replacement, Biochemistry 35 (1996) 10844–10853.

[14] P.Y. Chou, H.A. Scheraga, Calorimetric measurement of enthalpy change in the isothermal helix–coil transition of poly-L-lysine in aqueous solution, Biopolymers 10 (1971) 657–680.

[15] J. Hermans, Experimental free energy and enthalpy of formation of the α-helix, J. Phys. Chem. 70 (1966) 510–515.

[16] T. Ooi, M. Oobatake, Prediction of the thermodynamics of protein unfolding: the helix–coil transition of poly(L-alanine), Proc. Natl. Acad. Sci. USA 88 (1991) 2859–2863.

[17] G. Rialdi, J. Hermans, Calorimetric heat of the helix-coil transition of poly-L-glutamic acid, J. Am. Chem. Soc. 88 (1966) 5719–5720.

[18] J.M. Scholtz, R.L. Baldwin, The mechanism of α-helix formation by peptides, Annu. Rev. Biophys. Biomol. Struct. 21 (1992) 95–118.

[19] J.M. Scholtz, H. Qian, E.J. York, J.M. Stewart, R.L. Baldwin, Parameters of helix–coil transition theory for alanine-based peptides of varying chain lengths in water, Biopolymers 31 (1991) 1463–1470.

[20] J.M. Scholtz, S. Marqusee, R.L. Baldwin, et al., Calorimetric determination of the enthalpy change for the α-helix to coil transition of an alanine peptide in water, Proc. Natl. Acad. Sci. USA 88 (1991) 2854–2858.

[21] A.S. Ladokhin, S.H. White, Folding of amphipathic alpha-helices on membranes: energetics of helix formation by melittin, J. Mol. Biol. 285 (1999) 1363–1369.

[22] T. Wieprecht, O. Apostolov, M. Beyermann, J. Seelig, Interaction of a mitochondrial presequence with lipid

membranes: role of helix formation for membrane binding and perturbation, Biochemistry 39 (2000) 15297–15305.
[23] S. Rothemund, M. Beyermann, E. Krause, et al., Structure effects of double D-amino acid replacements: a nuclear magnetic resonance and circular dichroism study using amphipathic model helices, Biochemistry 34 (1995) 12954–12962.
[24] T. Wieprecht, O. Apostolov, J. Seelig, Binding of the antibacterial peptide magainin 2 amide to small and large unilamellar vesicles, Biophys. Chem. 85 (2000) 187–198.
[25] L.D. Mayer, M.J. Hope, P.R. Cullis, Vesicles of variable sizes produced by a rapid extrusion procedure, Biochim. Biophys. Acta 858 (1986) 161–168.
[26] T. Wiseman, S. Williston, J.F. Brandts, L.N. Lin, Rapid measurement of binding constants and heats of binding using a new titration calorimeter, Anal. Biochem. 179 (1989) 131–137.
[27] J. Seelig, Titration calorimetry of lipid-peptide interactions, Biochim. Biophys. Acta 1331 (1997) 103–116.
[28] R. Aveyard, D.A. Haydon, An Introduction to the Principles of Surface Chemistry, Cambridge University Press, London, 1973.
[29] S. McLaughlin, Electrostatic potentials at membrane–solution interfaces, Curr. Top. Membr. Transp. 9 (1977) 71–144.
[30] M.R. Wenk, J. Seelig, Magainin 2 amide interaction with lipid membranes: calorimetric detection of peptide binding and pore formation, Biochemistry 37 (1998) 3909–3916.
[31] T. Wieprecht, M. Beyermann, J. Seelig, Binding of antibacterial magainin peptides to electrically neutral membranes: thermodynamics and structure, Biochemistry 38 (1999) 10377–10387.
[32] C.R. Cantor, P.R. Schimmel, Biophysical Chemistry, Vol. 1, Freeman, San Francisco, 1980.
[33] G. Beschiaschvili, J. Seelig, Peptide binding to lipid bilayers. Nonclassical hydrophobic effect and membrane-induced pK shifts, Biochemistry 31 (1992) 10044–10053.
[34] J.A. Gazzara, M.C. Phillips, S. Lund-Katz, et al., Effect of vesicle size on their interaction with class A amphipathic helical peptides, J. Lipid Res. 38 (1997) 2147–2154.
[35] P. Luo, R.L. Baldwin, Mechanism of helix induction by trifluoroethanol: a framework for extrapolating the helix-forming properties of peptides from trifluoroethanol/water mixtures back to water, Biochemistry 36 (1997) 8413–8421.
[36] H. Heerklotz, J. Seelig, Detergent-like action of the antibiotic peptide surfactin on lipid membranes', Biophys. J. 81 (2001) 1547–1554.